AD-A072 876 NAVAL RESEARCH LAB WASHINGTON DC F/G 9/5
A MULTIPLE-BEAM MICROWAVE ANTENNA BASED ON THE PRINCIPLE OF THE--ETC(U)
APR 79 J F SIEBERT, L R MURPHY, T R LARSON

UNCLASSIFIED NRL-MR-3959 SBIE-AD-E000 309 NL

| OF |
AD
A072876

END
DATE
FILMED
9-79
DDC

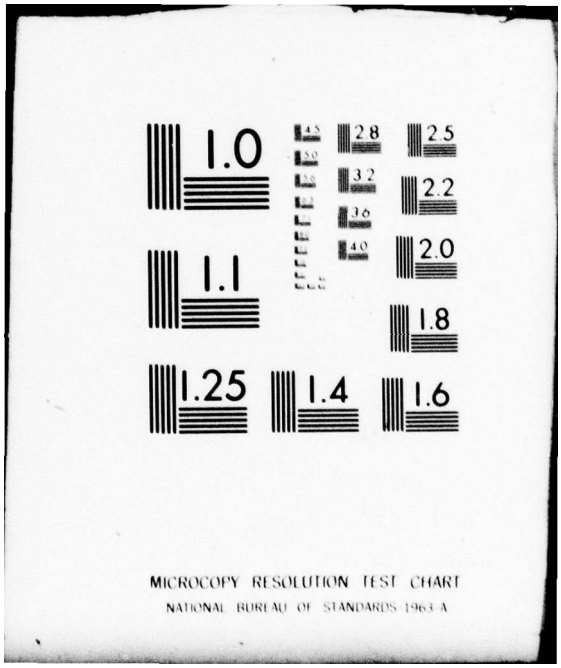
1.0
1.1
1.25
1.4
1.6
1.8
2.0
2.2
2.5
2.8
3.2
3.6
4.0
MICROCOPY RESOLUTION TEST CHART
NATIONAL BUREAU OF STANDARDS-1963-A

NRL Memorandum Report 3989



# A Multiple-Beam Microwave Antenna Based on the Principle of the Mills Cross

J. F. SIEBERT, L. R. MURPHY, T. R. LARSON

*Ball Aerospace Systems Division*
*Boulder, Colorado*

and

J. P. HOLLINGER

*Advanced Space Sensing Applications Branch*
*Space Science Division*



April 3, 1979





NAVAL RESEARCH LABORATORY
Washington, D.C.

SECURITY CLASSIFICATION OF THIS PAGE (When Data Entered)

| REPORT DOCUMENTATION PAGE | | READ INSTRUCTIONS BEFORE COMPLETING FORM |
|---|---|---|
| 1. REPORT NUMBER<br>NRL Memorandum Report 3959 | 2. GOVT ACCESSION NO. | 3. RECIPIENT'S CATALOG NUMBER |
| 4. TITLE (and Subtitle)<br>A MULTIPLE – BEAM MICROWAVE ANTENNA BASED ON THE PRINCIPLE OF THE MILLS CROSS | | 5. TYPE OF REPORT & PERIOD COVERED<br>Progress Report<br>6. PERFORMING ORG. REPORT NUMBER |
| 7. AUTHOR(s)<br>J. F. Siebert*, L. R. Murphy*, T. R. Larson*, and J. P. Hollinger | | 8. CONTRACT OR GRANT NUMBER(s) |
| 9. PERFORMING ORGANIZATION NAME AND ADDRESS<br>Naval Research Laboratory<br>Washington, D.C. 20375 | | 10. PROGRAM ELEMENT, PROJECT, TASK AREA & WORK UNIT NUMBERS<br>NRL Problem G01-10<br>62759N<br>Project WF52-553-701 |
| 11. CONTROLLING OFFICE NAME AND ADDRESS<br>Naval Air Systems Command<br>Surveillance Administrator (AIR 370)<br>Washington, D.C. 20715 | | 12. REPORT DATE<br>April 3, 1979<br>13. NUMBER OF PAGES<br>56 |
| 14. MONITORING AGENCY NAME & ADDRESS(if different from Controlling Office) | | 15. SECURITY CLASS. (of this report)<br>UNCLASSIFIED<br>15a. DECLASSIFICATION/DOWNGRADING SCHEDULE |

16. DISTRIBUTION STATEMENT (of this Report)

Approved for public release; distribution unlimited.

17. DISTRIBUTION STATEMENT (of the abstract entered in Block 20, if different from Report)

18. SUPPLEMENTARY NOTES

*Ball Aerospace Systems Division, Boulder, Colorado

19. KEY WORDS (Continue on reverse side if necessary and identify by block number)

Unfilled aperture
Remote sensing
Microwave radiometry
Mills cross
Multiple beam antennas

20. ABSTRACT (Continue on reverse side if necessary and identify by block number)

A study has been carried out to determine the feasibility of various antenna configurations for a proposed satellite mission to profile the surface temperature of the ocean using a passive microwave radiometer. Specifically, a static, multiple-beam microwave antenna utilizing a phase-switched Mills cross as its basic element is proposed and analyzed in detail. Although the Mills cross configuration does not completely meet the specified requirements of this particular application, its analysis does provide a necessary frame of reference for assessing its usefulness in general, and for establishing its features and drawbacks relative to alternative antenna configurations. It also
(Continues)

DD FORM 1 JAN 73 1473 EDITION OF 1 NOV 65 IS OBSOLETE
S/N 0102-014-6601

20. Abstract (Continued)

serves as an illustrative example of some of the design tradeoffs and problems that are encountered in trying to map the earth's surface from a space platform.

CONTENTS

# A MULTIPLE-BEAM MICROWAVE ANTENNA BASED ON THE PRINCIPLE OF THE MILLS CROSS

## I. Introduction

Remote sensing of geophysical and climatic parameters using microwave radiometers has become increasingly attractive with the advent of the payload capabilities of the space shuttle[1]. However, to achieve comparable resolution, space mounted radiometers must have antennas more than an order of magnitude larger than their aircraft mounted counterparts. For instance, 1 km resolution at 500 km range requires $\sim$ 20 m antenna extent at 10 GHz.

Although the compatibility of such large antennas with conventional radiometric imaging systems and techniques has recently been considered from the point of view of integration time, bandwidth, and antenna losses,[2] no attempt was made to assess the impact of specific antenna configurations on the space platform itself. Since the size and mass of a large antenna can easily exceed those of the spacecraft, the range of factors used to determine a given antenna design and operating mode must be broadened to include the size, mass, and configurational constraints imposed by the space platform.

This paper is a report on some aspects of a study carried out to determine the feasibility of various antenna configurations for a proposed Remote Ocean-Surface Measurement System (ROMS) mission to profile the surface temperature of the ocean using a passive microwave radiometer. In particular, a static, multiple-beam, microwave antenna utilizing a phase-switched Mills cross[3]

Note: Manuscript submitted January 19, 1979.

as its basic element is proposed and analyzed in detail. Although the Mills cross configuration does not completely meet the specified requirements of this particular application, its analysis does provide a necessary frame of reference for assessing its usefulness in general, and for establishing its features and drawbacks relative to alternative antenna configurations. It also serves as an illustrative example of some of the design tradeoffs and problems that are encountered in trying to map the earth's surface from a space platform.

The paper is organized as follows. In Section II the ROMS mission objectives and parameters are defined, and some of the configurational and operational tradeoffs that led to an antenna design based on the Mills cross are discussed. In Section III the basic theory of the phase-switched Mills cross and of some of its variations is presented, and then is used to predict the performance of a phased and tilted-arm configuration necessary for the ROMS application. In Section IV the beam stacking and data processing procedures necessary for optimum image restoration are specified. The final configurational tradeoffs are then made in order to design and then assess the predicted performance of a Mills cross multiple-beam antenna in terms of the ROMS mission requirements. A discussion and our conclusions are given in Section V.

## II. ROMS Mission Configuration and Parameters

The ocean surface is an extended source of electromagnetic radiation, whose radiation properties, at a given frequency and polarization, can be fully characterized by a brightness tempera-

ture, $T_B(\theta,\phi)$.[4] The ROMS mission is to map $T_B(\theta,\phi)$ using a passive microwave radiometer mounted on a satellite platform, as is schematically illustrated in Figure 1 for the case of a single beam Mills cross antenna. Most of the parameters necessary to specify the mission and the antenna design are defined in this figure, and a representative set of values are included (in parentheses) for perspective. The basic surface temperature measurement is made at 6 GHz. Other higher frequency channels are used to correct for ocean roughness and intervening atmospheric effects and require a much smaller aperture antenna than the 6 GHz channel. At 6 GHz, the basic system requirements are 10 km resolution, 500 km swath width, and a $0.5^{\circ}K$ system sensitivity to sea surface temperature. In addition, the measurements are restricted to vertically polarized radiation at approximately a 55 degree angle of incidence with the sea surface, in order to reduce the dependence of $T_B(\theta,\phi)$ on ocean roughness effects[5] and to maximize the dependence on sea surface temperature.

The high resolution temperature profile transverse to the satellite motion might be achieved by either a mechanically scanned single beam antenna, or by using a static multiple-beam configuration. A mechanically scanned parabola is simple conceptually, but would require a sophisticated mechanical drive in order to scan such a large antenna without significantly disturbing the stability of the space platform. It also has the disadvantage of a much shorter effective integration time relative to a static multiple-beam configuration, since tht <u>total</u> available integration time for profiling a 10 km by 500 km transverse strip

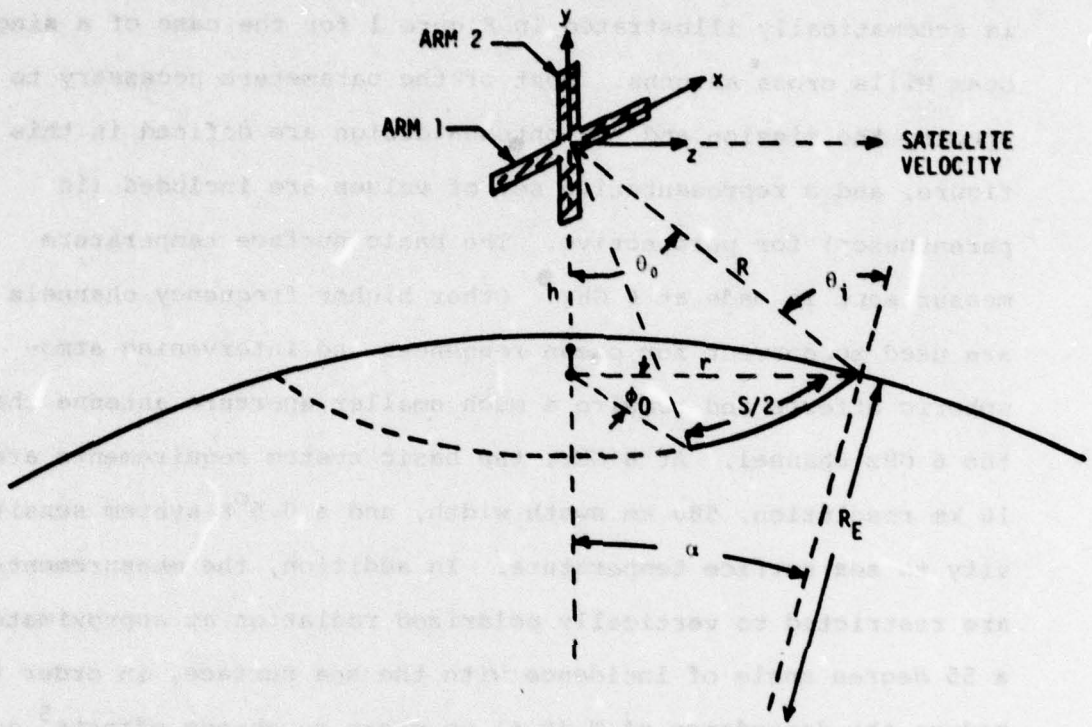


| GIVEN PARAMETERS | DERIVED PARAMETERS |
|---|---|
| $h_0$ = ALTITUDE (500 km) | h = EFFECTIVE ALTITUDE (530 km) |
| $\theta_i$ = INCIDENCE ANGLE (55°) | R = SLANT RANGE (815 km) |
| S = SWATH WIDTH (500 km) | r = HORIZONTAL RANGE (620 km) |
| $R_E$ = RADIUS OF EARTH (6370 km) | $\theta_0$ = VERTICAL BEAM SWING (49.5°) |
| | $\phi_0$ = MAXIMUM HORIZONTAL BEAM SWING (23°) |
| | α = EARTH SUBTENDED ANGLE (5.5°) |

**Fig. 1 - The ROMS mission parameters. A representative set of values is given in parentheses.**

of ocean is limited by the satellite motion ($\sim$ 1.4 seconds for a 500 km circular orbit). On the other hand, the classical techniques for simultaneous beam forming in a static configuration (e.g., microwave lenses, microwave networks, and IF beam forming[6]) are quite complicated, both analytically and mechanically. In particular, it is difficult to adapt these configurations to the size and mass constraints of a space platform, and each contains large insertion losses that essentially negate the advantage in integration time.

For these reasons, it was decided to try a new approach to the design of a static multiple-beam antenna using the principle of the Mills cross. In this discussion, the terminology Mills cross is used to characterize that particular class of phase-switched interferometers where the two (rectangular) apertures are in physical contact. This ranges from the symmetrical cross to the tee or ell configurations, as shown in Figure 2. Also shown are the sensitivity expression and far-field resolution pattern (the dotted lines) for each configuration except the ell. As will be demonstrated, the phase-switched Mills cross has the property, of an unfilled aperture, that the sensitivity can be varied independently of the resolution. The resolution in a given direction is determined by the effective antenna extent in that direction, and is established by hypothetically symmetrizing each configuration, as is illustrated by the dashed lines in Figure 2. Sensitivity is then preserved by balancing any increase in resolution with a corresponding increase in arm width (receiving area). Consequently, it is possible to achieve a rough equivalence

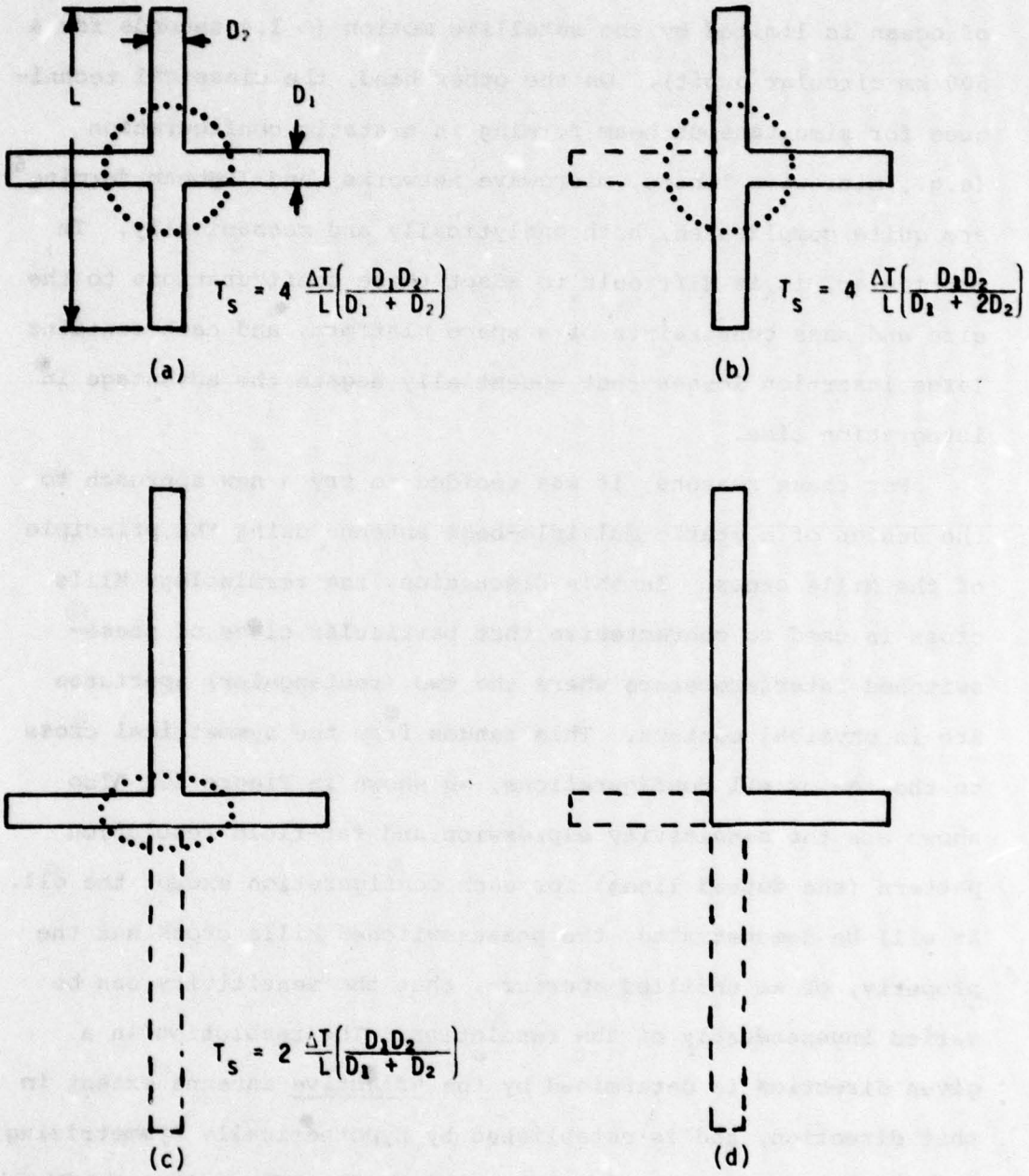


**Fig. 2 - Four variations of the Mills cross using a common vertical arm. The dashed lines used to symmetrize each configuration establish the effective antenna arm lengths. The dotted lines represent the far-field resolution patterns of each configuration except the ell, and $T_S$ is the expression for the corresponding sensitivity.**

in the sensitivity and resolution of each of these configurations, and, therefore, it is reasonable to consider the possiblity of stacking them together to from a compact multiple-beam antenna. This approach is relatively simple, both conceptually and mechanically, since the final antenna configuration, as shown in Figure 3, is basically a stacked arrangement of many static single-beam antennas. A detailed design and performance analysis of this general configuration in terms of the ROMS mission requirements is the subject of the remainder of this paper.

## III. Theory of the Mills Cross

### A. General Description

When a two aperture antenna is rapidly switched between the in-phase (+) and out-of-phase (-) operating modes, the antenna output has a modulation superimposed of amplitude

$$T_s = T_{A+} - T_{A-} \quad , \tag{1}$$

where the antenna temperature is related to the source brightness temperature through the convolution with the antenna power pattern[7]

$$T_{A\pm}(\theta,\phi) = \frac{\int P_{\pm}(\theta-\theta',\phi-\phi')\ T_B(\theta',\phi')\ d\Omega'}{\int P_{\pm}(\theta,\phi)\ d\Omega} \quad . \tag{2}$$

For the particular case where the two apertures have common centers, i.e., the symmetric Mills cross, the antenna power pattern, $P_{\pm}(\theta,\phi)$, is simply related to the far-field patterns, $E(\theta, \phi)$, of each aperture through the relationship

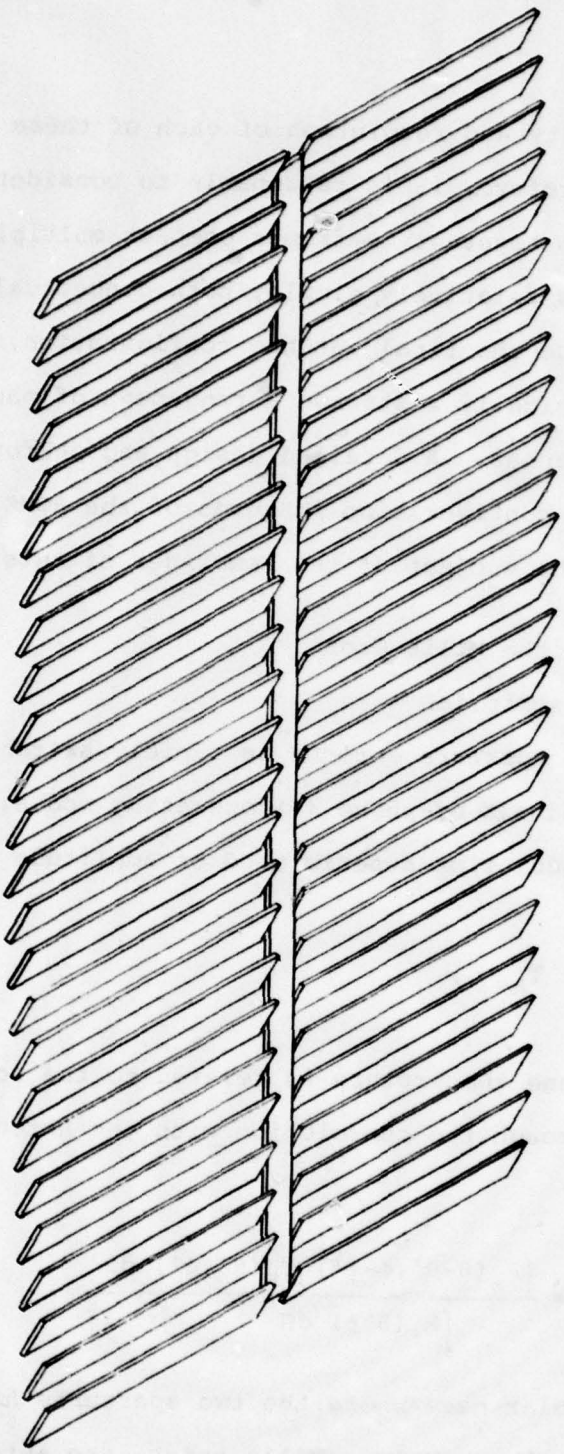

**Fig. 3 - A 25 beam, tilted-horizontal-arm, Mills cross antenna that utilizes a common vertical arm. A detailed theoretical design and performance analysis of this particular configuration in terms of the ROMS mission requirements is given in Figure 12.**

$$P_{\pm} = E_{\pm}E_{\pm}^{*} = (E_1 \pm E_2)(E_1 \pm E_2)^{*} = |E_1|^2 + |E_2|^2 \pm (E_1 E_2^{*} + E_1^{*} E_2), \quad (3)$$

where the subscript 1(2) refers to aperture 1(2). It is also useful to refer variations in the source brightness temperature to the "average" temperature of the extended source over the entire region sensed by $P_{\pm}(\theta,\phi)$ through the equation

$$T_B(\theta,\phi) = T_B(\text{ave}) + \Delta T_B(\theta,\phi), \quad (4)$$

where $\Delta T_B(\theta,\phi)$ is defined such that

$$\int (|E_1|^2 + |E_2|^2)\ \Delta T_B\ d\Omega = 0. \quad (5)$$

Eqs. (1)-(5) can then be combined to yield the general relationships

$$T_B(\text{ave}) = \frac{T_{A+} + T_{A-}}{2}, \quad (6)$$

and

$$T_S = \frac{2}{\Omega_1 + \Omega_2} \int (E_1 E_2^{*} + E_1^{*} E_2)\ \Delta T_B\ d\Omega, \quad (7)$$

where the (unnormalized) solid angles of each beam and the correlation region are defined by

$$\Omega_1 = \int |E_1|^2\ d\Omega, \quad (8a)$$

$$\Omega_2 = \int |E_2|^2 \, d\Omega \ , \tag{8b}$$

$$\Omega_c = \int \frac{(E_1 E_2^* + E_1^* E_2)}{2} \, d\Omega \ . \tag{8c}$$

In deriving Eqs. (6) and (7), it was assumed that the correlation region is small, so that terms down by a factor $[\Omega_c/(\Omega_1+\Omega_2)]^2$ could be neglected.

On the basis of the discussion so far, three general observations about the properties of phase-switched Mills crosses can be made:

- Any component of $T_B(\theta,\phi)$ which is constant over the entire solid angle for which $P_\pm$ exists does not contribute to $T_s$. Equivalently, the DC spatial frequency response of such an antenna is zero.
- $T_s$ is the convolution of $\Delta T_B$ with an "effective" antenna power pattern proportional to the product of the far-fields of each aperture of the interferometer. Therefore, the resolution in measuring $\Delta T_B$ is determined by the far-field correlation region, which is characterized by the solid angle, $\Omega_c$.
- In general, $T_B$(ave) varies with time, and must be measured indpendently with an accuracy comparable to that for $T_s$. The difficulty in making this measurement depends on the magnitude and rate of the fluctuations in $T_B$(ave). Only if these variations are relatively small and slow is the phase-switched Mills

cross useful for high accuracy, high resolution measurements on extended sources.

The significance of these observations is best illustrated by considering the simple example of a uniformly excited, symmetric Mills cross, as shown in Figure 4. Each arm has a fan shaped far-field pattern as shown, where the vertical arm produces the horizontal beam, and vice versa. By periodically phase-switching the two arms, a modulated output signal of amplitude $T_s$ is produced that is determined only by those particular brightness temperature deviations from the overall average that occur in the (cross-hatched) region common to both beams. Using equations 7 and 8 and simple geometric arguments, it is evident that the antenna sensitivity has the qualitative dependence

$$T_s \sim \frac{D}{L} \Delta T \ . \qquad (9)$$

This result shows that the sensitivity can be varied independently of the resolution by making appropriate adjustments in the D/L ratio. Therefore, for those applications where the average background temperature is at most a slowly varying function of time, so that it can be easily and accurately measured independently, the effective resolution of the Mills cross corresponds to the cross-hatched region shown and is determined entirely by the lengths of the antenna arms. In the ROMS application it is possible that occasional rapid variations in $T_B$(ave) might occur. For instance, a sudden encounter of one of the beam arms with a

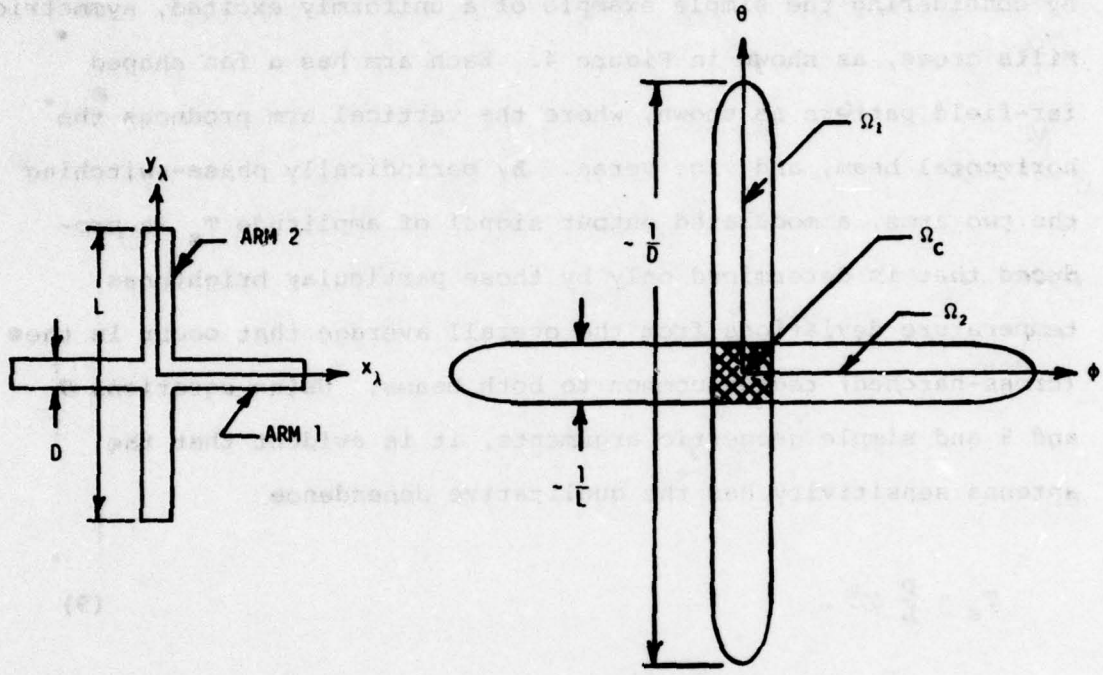


UNIFORMLY EXCITED MILLS CROSS

FAR-FIELD POWER PATTERNS

$$\text{RESOLUTION} \sim \frac{1}{L}$$

$$T_s \sim \frac{\Omega_c}{\Omega_1 + \Omega_2}\,\Delta T \sim \frac{\frac{1}{L^2}}{\frac{1}{DL} + \frac{1}{DL}}\,\Delta T \sim \frac{D}{L}\,\Delta T$$

**Fig. 4 - Qualitative description of the resolution and sensitivity of a uniformly excited Mills cross antenna. Using geometrical arguments, it is evident that the resolution (cross-hatched area) is inversely proportional to antenna extent, L, and the sensitivity has the qualitative dependence $T_s \sim (D/L)\,\Delta T$, where $\Delta T$ is the temperature deviation of the source within the cross-hatched region.**

land mass would produce an abrupt change in $T_B$(ave) and a corresponding equal and opposite change in $T_s$, even though the actual brightness temperature in the correlation region remained constant. This possibility must be taken into account in designing a system to monitor $T_B$(ave).

B. Aperture Excitation and Far-Field Radiation Pattern

A quantitative determination of the resolution and sensitivity of a given antenna configuration requires knowledge of the far-field radiation patterns, $E(\theta,\phi)$, as determined by the distribution and level of excitation in the corresponding apertures. In practice, the apertures are composed of arrays of discrete elements, appropriately excited and phased to produce the desired far-field power patterns. A particularly simple model of an aperture array is one composed of many electric (or magnetic) dipoles, so small and so closely spaced that the far-field structure due to the discreteness of the elements is not resolved. In this limit, the aperture is effectively a current sheet, whose radiating properties can be conveniently characterized by a continuous electric field distribution, $\varepsilon(x_\lambda,y_\lambda)$, over the plane of the aperture. For the present purpose of assessing the relative performance of various antenna configurations, this simplified description is adequate.

Assuming a vertically polarized aperture distribution, $\varepsilon_y(x_\lambda,y_\lambda)$, the corresponding far-field pattern is determined by the Fourier transform relationship[8,9]

$$\varepsilon_y(x_\lambda, y_\lambda) = \int_{-\infty}^{\infty}\int_{-\infty}^{\infty} \frac{n}{(1-\ell^2)^{(1/2)}} E(\ell,m) e^{i2\pi(\ell x_\lambda + m y_\lambda)} d\ell dm \ , \quad (10a)$$

and

$$\frac{n}{(1-\ell^2)^{1/2}} E(\ell,m) = \int_{-\infty}^{\infty}\int_{-\infty}^{\infty} \varepsilon_y(x_\lambda, y_\lambda)\ e^{-i2\pi(\ell x_\lambda + m y_\lambda)} dx_\lambda dy_\lambda \ , \quad (10b)$$

where $E(\ell,m)$ is the far-field of the ray$(\ell,m)$, and the subscript "$\lambda$" indicates that all dimensions are expressed in wavelengths $(\ell,m,n)$ are the direction cosines

$$\ell = -\sin\theta \sin\phi, \quad (11a)$$

$$m = -\cos\theta, \quad (11b)$$

$$n = \sin\theta \cos\phi, \quad (11c)$$

where $\theta$ defines the beam position relative to nadir, and $\phi$ is the horizontal angular deviation of the beam away from broadside, as shown in Figure 1. Eq. (1) is not quite the classical Fourier transformation because of the factor $n/(1-\ell^2)^{1/2}$, which is just the cosine of the angle between $E(\ell,m)$ and the polarization direction. Therefore, the definition

$$E_y(\ell,m) = \frac{n}{(1-\ell^2)^{1/2}}\ E(\ell,m) \quad (12)$$

establishes $\varepsilon_y(x_\lambda, y_\lambda)$ and $E_y(\ell,m)$ as a standard Fourier transform pair, where $E_y(\ell,m)$ is just the vertical component of $E(\ell,m)$.

The corresponding power radiation pattern, defined as the power radiated in a given direction per unit solid angle, can be written

$$|E(\theta,\phi)|^2 = \frac{|E(\ell,m)|^2\, d\ell dm}{d\Omega} = n|E(\ell,m)|^2 = \frac{(1-\ell^2)}{n}\,|E_y(\ell,m)|^2. \quad (13)$$

For a highly directive antenna radiating close to the broadside direction (i.e., $(1-\ell^2)/n \sim 1$), the aperture polarization can be neglected and $|E_y(\ell,m)|^2$ is essentially the same as the power radiation pattern. However, for non-broadside operation, there is a strong dependence of the power radiated upon the scan angle.

To illustrate this dependence, consider an antenna with a broadside radiation pattern $E(\theta,\phi) \cong E_y(\ell,m)$ that has been phased to produce the shifted pattern $E_y(\ell-\ell_o, m-m_o)$ centered about the direction $(\ell_o, m_o)$. The required aperture excitation level and phasing is obtained by applying the shift theorem[9] to the original aperture distribution, i.e.,

$$\epsilon_y(x_\lambda, y_\lambda)\; e^{-i2\pi(\ell_o x_\lambda + m_o y_\lambda)} \supset E_y(\ell-\ell_o, m-m_o), \quad (14)$$

where the symbol "$\supset$" is used to relate these quantities as a Fourier transform pair. This result states that uniform phase gradients of $\ell_o = -\sin\theta_o \sin\phi_o$ and $m_o = -\cos\theta_o$ cycles per wavelength along the $x_\lambda$- and $y_\lambda$-directions, respectively, produce the desired beam swing from broadside to $(\theta_o, \phi_o)$. For a highly directive antenna, the <u>total</u> power radiated as a function of the scan angles can then be written

$$\int |E(\theta-\theta_o, \phi-\phi_o)|^2 \, d\Omega = \int \frac{1-\ell^2}{n} \, |E_y(\ell-\ell_o, m-m_o)|^2 \, \frac{d\ell dm}{n}$$

$$\simeq \frac{1-\ell_o^2}{n_o^2} \int |E_y(\ell,m)|^2 \, d\ell dm, \qquad (15)$$

which states that, for a given aperture excitation level, the total radiated power varies as $(1-\ell_o^2)/n_o^2$.

This predicted variation in total radiated power with scan angle can be attributed to two factors. The first is that the antenna input impedance varies in inverse proportion to $(1-\ell_o^2)/n_o$.[10,11] Consequently, for the "forced" excitation of fixed amplitude assumed in Eq. (14), a dependence of the total radiated power on this factor is expected. In practice, the antenna excitation is free rather than forced, and this effect can be eliminated by proper impedance matching of the receiver to the antenna for a given scan angle. The remaining inverse dependence of the total radiated power on $n_o = \sin\theta \cos\phi$ is related to the reduction in the effective aperture size with increasing scan angle. By increasing the vertical aperture dimension by $1/\sin\theta_o$, and the horizontal dimension by $1/\cos\phi_o$, the effective aperture is independent of scan angle and this dependence is eliminated.

C. Asymmetrical Aperture Distributions

The sensitivity expression, Eq. (7), is restricted to phase-switched interferometers whose apertures have a common center. This includes the symmetrical Mills cross, but apparently excludes its variations, such as the tee or the ell. However, Figure 5a illustrates that any two (rectangular) aperture an-

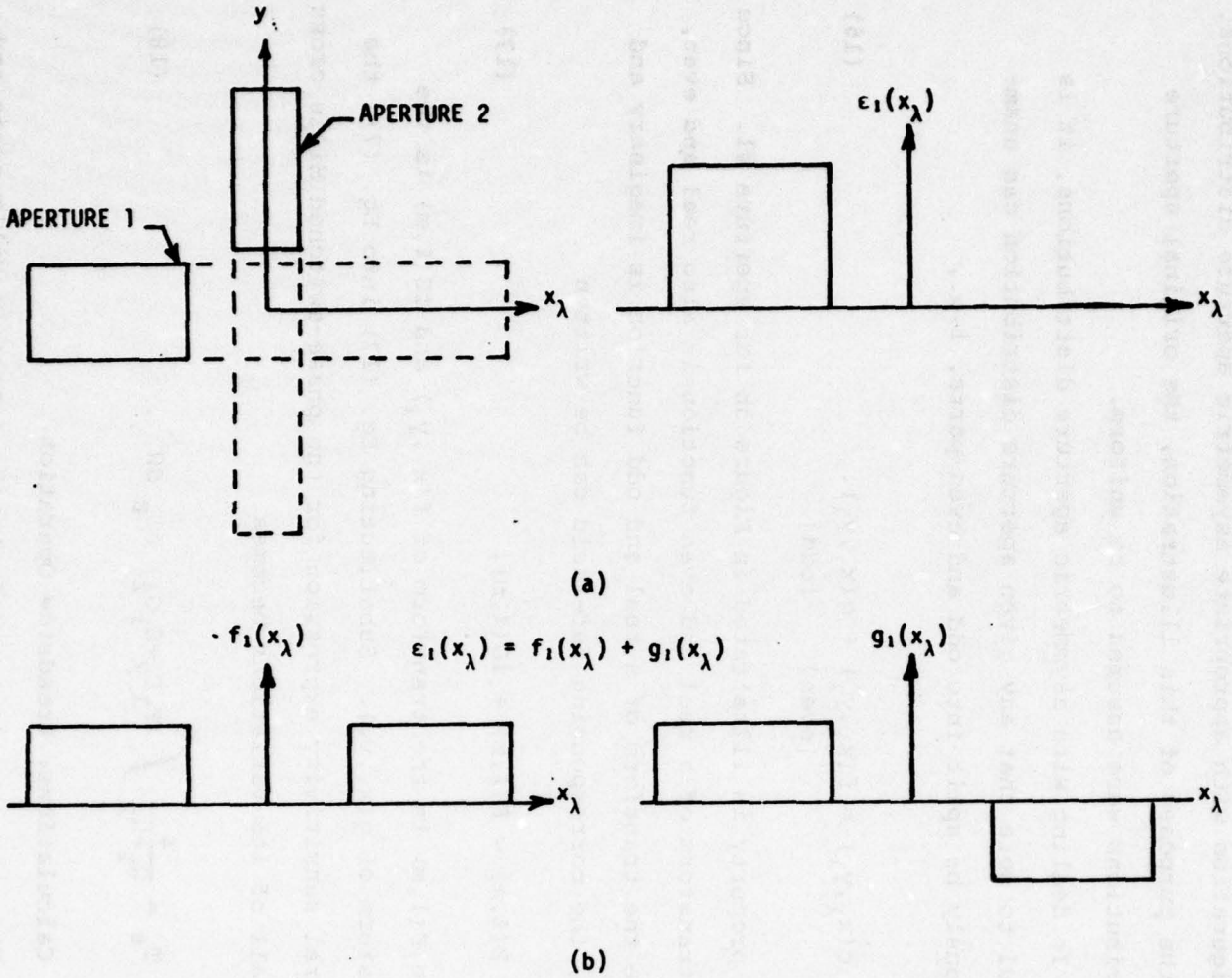


Fig. 5 - (a) Asymmetric aperture excitation distribution characterizing a "symmetrized" arm of a two aperture antenna. (b) Asymmetric aperture distribution split into its odd and even components.

tennae with real and symmetric aperture distributions (as is usually the case) can be replaced by the classic Mills cross configuration with appropriate asymmetric aperture distributions. For the purposes of this illustration, the original aperture distributions were assumed to be uniform.

In dealing with asymmetric aperture distributions, it is useful to note that any given aperture distribution can unambiguously be split into odd and even parts, i.e.,

$$\underset{}{\varepsilon(x_\lambda,y_\lambda)} = \underset{[\text{even}]}{f(x_\lambda,y_\lambda)} + \underset{[\text{odd}]}{g(x_\lambda,y_\lambda)}. \tag{16}$$

This property is illustrated in Figure 5b for aperture #1. Since the transform of a real and even function is also real and even, while the transform of a real and odd function is imaginary and odd[9], the corresponsing far-field can be written

$$E(\ell,m) = F(\ell,m) + iG(\ell,m), \tag{17}$$

where $F(l,m)$ is the transform of $f(x_\lambda,y_\lambda)$ and $iG(\ell,m)$ is the transform of $g(x_\lambda,y_\lambda)$. Substituting Eq. (17) into Eq. (7), the general sensitivity expression for the phase-switched Mills cross and all of its variations becomes

$$T_s = \frac{4}{\Omega_1+\Omega_2} \int (F_1F_2+G_1G_2)\ \Delta T_B\ d\Omega \quad . \tag{18}$$

D. Calculations: Broadside Operation

The next step is to evaluate the symmetric Mills cross and some of its variations as possible elements in a multiple-beam

configuration. For this purpose, it is both convenient and sufficient to assume uniformly excited, high directivity apertures radiating in the broadside direction, so that $\varepsilon(x_\lambda, y_\lambda)$ and $E(\ell,m)$ are approximately a Fourier transform pair. Then applying Eq. (10) to the case of a uniformly excited rectangular aperture of width D and length L (in wavelengths) yields the approximate result

$$\varepsilon(x_\lambda, y_\lambda) = \prod\left(\frac{x_\lambda}{D}\right)\prod\left(\frac{y_\lambda}{L}\right) \supset E(\ell,m) = DL \text{ sinc } D\ell \text{ sinc } Lm, \tag{19}$$

where the rectangle function

$$\prod(x) = \begin{cases} 0 & |x| > 1/2 \\ 1 & |x| < 1/2 \end{cases} \tag{20}$$

has been used to characterize a uniform excitation of unit amplitude.

Case 1. Symmetric Mills Cross (Figure 2a)

For generality, the arms are permitted to have different widths and lengths. From Eq. (19),

$$E_1(\ell,m) = D_1L_1 \text{ sinc } L_1\ell \text{ sinc } D_1m, \tag{21a}$$

$$E_2(\ell,m) = D_2L_2 \text{ sinc } D_2\ell \text{ sinc } L_2m. \tag{21b}$$

The antenna sensitivity and spatial frequency response in a given direction are found by assuming a sinusoidal disturbance in that direction, and then applying the sensitivity expression, Eq.

(7). For instance, in the far-field direction conjugate to $x_\lambda$ we assume

$$\Delta T_B(\ell,m) = \Delta T \cos 2\pi f \ell \simeq \Delta T \cos 2\pi f_\phi \phi \ , \qquad (22)$$

where $\phi$ is the (assumed small) angular deviation from the broadside direction, $f_\phi$ is the corresponding spatial frequency in cycles/radian, and $\Delta T$ is the oscillation amplitude. Performing the required integrals yields

$$T_s(f_\phi) = \begin{cases} 4\ \Delta T\ \dfrac{D_1 D_2}{L_1 D_1 + L_2 D_2} & f_\phi < \dfrac{L_1 - D_2}{2} \\ 4\ \Delta T\ \dfrac{D_1 D_2}{L_1 D_1 + L_2 D_2} \left[ \dfrac{(L_1 + D_2) - 2 f_\phi}{2 D_2} \right] & \dfrac{L_1 - D_2}{2} < f_\phi < \dfrac{L_1 + D_2}{2} \\ 0 & f_\phi > \dfrac{L_1 + D_2}{2} \end{cases} \qquad (23)$$

Note that the spatial frequency cutoff (resolution) in a given direction is determined primarily by the length of the arm in that direction. This expression can be simplified by assuming isotropic resolution ($L_1 = L_2 = L$), and narrow arm widths ($L \gg D_1, D_2$). Then the high frequency rolloff can be neglected, and Eq. (23) reduces to the flat sensitivity response

$$T_s(f_\phi) \simeq 4\Delta T\ \frac{1}{L}\ \frac{D_1 D_2}{D_1 + D_2} \qquad f_\phi < \frac{L}{2} \qquad (24)$$

up to the cutoff frequency, $f_c = L/2$. Note that the arm widths enter the sensitivity expression in parallel, and should be kept roughly equal to maximize sensitivity.

The flat spatial frequency response predicted above for the Mills cross in the $\phi$-direction is ideal for optimum image restoration of an extended source. By definition, the antenna sensitivity is constant for each spatial frequency component out to a well-defined cutoff, which can be directly related to the real space resolution of the extended source mapping. Note, however, that the response of the Mills cross is not isotropic. This is illustrated by the three response curves shown in Figure 6, corresponding to different far-field directions. Only in the high symmetry $\phi$ and $\theta$ far-field directions conjugate to $x_\lambda$ and $y_\lambda$ is the response ideal, as shown in Figure 6a. In fact, at 45 degrees to these directions, the response has the triangular shape characteristic of a uniformly excited filled array (Figure 6c). Therefore, optimum image restoration is achieved with a Mills cross only if its orientation is chosen so that the scan and/or multiple-beam sampling directions coincide with the $\phi$ or $\theta$ far-field directions.

Although the Mills cross has a flat spatial frequency response for certain orientations, it is the exception. Most antennas, like the Mills cross for arbitrary orientations, have responses that are less than ideal, so that the meanings of extended source antenna sensitivity and real space resolution are not clearly defined. Yet, adequate definitions are vital if one wants to compare the performances of different antennas and to do design tradeoffs. An approximate remedy to this situation is achieved by defining an <u>equivalent</u> ideal flat spatial frequency response curve in each case, as is illustrated by the dotted line

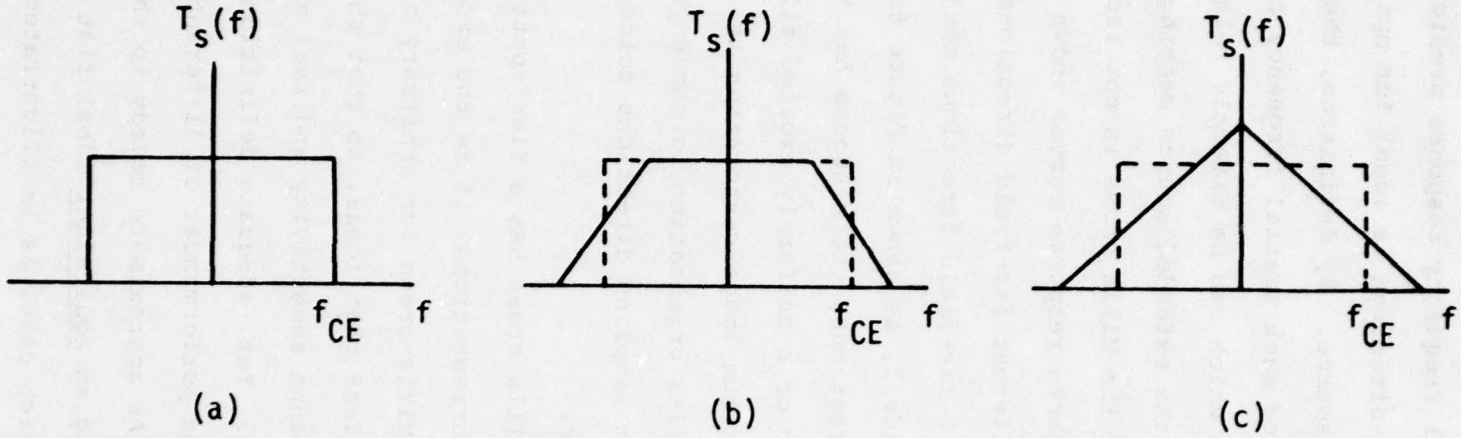


Fig. 6 - Spatial frequency response of an ideal, uniformly excited, symmetrical Mills cross in (a) the high symmetry $\theta$ (or $\phi$) far-field direction, (b) $26.5^{o}$ from $\theta$ (or $\phi$), and (c) $45^{o}$ from $\theta$ (or $\phi$). In each case, the dotted line rectangle is the <u>equivalent</u> flat spatial frequency response, as defined in the text.

rectangles shown in Figure 6. Specifically, the equivalent ideal cutoff frequency, $f_{ce}$, is defined by the weighted average

$$f_{ce} = \frac{\int_0^{T_s(0)} [f(T_s)]^2 \, dT_s}{\int_0^{T_s(0)} f(T_s) \, dT_s} \tag{25}$$

where $f(T_s)$ is the inversion of $T_s(f)$ (i.e., the integration is carried out along the vertical axis). Applying this definition to the uniformly excited Mills cross yields the isotropic equivalent spatial frequency response, and, hence, the circular real space resolution pattern shown in Figure 2a. The corresponding isotropic sensitivity expression is given by Eq. (24).

Additional support for the definition, Eq. (25), is found by noting that, for a given aperture distribution, the equivalent cutoff frequencies of the Mills cross and the filled array are both inversely related to the 3 dB widths of the corresponding power patterns through the same proportionality constant. More specifically, this definition requires that, for the same aperture distribution, the Mills cross must have an extent $\sim\sqrt{2}$ greater than that of a filled aperture in order to have the same resolution. This is a significant consideration in weighing the relative merits of the single-beam, mechanically scanned, filled aperture approach to the ROMS mission against the Mills cross, multiple-beam, static approach. It should be noted that Eq. (25) is useful only as long as $T_s(0)$ represents the peak sensi-

tivity. This is usually the case for antenna configurations and aperture distributions used to observe extended sources.

Case 2. Symmetric (Equal Arm) Tee (Figure 2b)

The antenna is first physically symmetrized by introducing the appropriate asymmetrical aperture distribution for the horizontal arm (Aperture #1). Since the vertical arm is already symmetrical,

$$\varepsilon_1(x_\lambda, y_\lambda) = \frac{1}{2}\prod\left(\frac{x_\lambda}{L}\right)\prod\left(\frac{y_\lambda}{D_1}\right) + \frac{1}{2}\left[\prod\left(\frac{2x_\lambda}{L} - \frac{1}{2}\right) - \prod\left(\frac{2x_\lambda}{L} + \frac{1}{2}\right)\right]\prod\left(\frac{y_\lambda}{D_1}\right), \quad (26a)$$

$$\varepsilon_2(x_\lambda, y_\lambda) = \prod\left(\frac{x_\lambda}{D_2}\right)\prod\left(\frac{y_\lambda}{L}\right) . \quad (26b)$$

The corresponding far-field patterns are

$$E_1(\ell,m) = \frac{D_1 L}{2}\,\text{sinc}\, L\ell\,\text{sinc}\, D_1 m - \frac{iD_1 L}{2}\,\text{sinc}\,\frac{L}{2}\ell\,\sin\pi\,\frac{L}{2}\ell\,\text{sinc}\, D_1 m , \quad (27a)$$

$$E_2(\ell,m) = D_2 L\,\text{sinc}\, D_2\ell\,\text{sinc}\, Lm . \quad (27b)$$

On applying Eq. (18), it is immediately evident that the correlated power pattern, and, hence, the resolution, of a symmetric tee is identical to that of a symmetric cross of the same extent. This is because the asymmetric field $G_1$ does not contribute as long as $G_2 = 0$. However, because $G_1$ is non-zero and large, any asymmetries in the vertical arm will now result in first order deviations in the antenna response, and could present practical difficulties[3]. The corresponding sensitivity expression for the tee is

$$T_s(f) = 4\,\Delta T\,\frac{1}{L}\left[\frac{D_1 D_2}{D_1+2D_2}\right] \qquad f < \frac{L}{2}\ , \tag{28}$$

which is somewhat different from that of the cross. In particular, if $D_1 = D_2 = D$ for the cross, then it is required that $D_1 = 2D_2 = 2D$ for the tee to have equal sensitivity. This means that the cross and tee must have equal receiving areas in order to have equal sensitivities.

Case 3. Asymmetric Cross (Figure 2c)

This configuration is essentially a tee with unequal arms. Applying similar formalism to this configuration yields the anisotropic response

$$T_s(f) = 2\,\Delta T\,\frac{1}{L}\left[\frac{D_1 D_2}{D_1 + D_2}\right] \qquad \begin{matrix} f_\phi < \frac{L}{2} \\ f_\theta < L \end{matrix}\ . \tag{29}$$

The different cutoff frequencies indicate that the corresponding real space resolution is elliptical, as shown in Figure 2c, where the resolution along the vertical arm is twice that along the horizontal arm. Because of this anisotropic increase in resolution, there is a factor of two loss in sensitivity relative to the symmetric cross when the arm widths of both configurations are equal. Note that <u>both</u> $D_1$ and $D_2$ must be doubled in order to recover this drop in sensitivity.

Case 4. The Ell (Figure 2d)

Using the above formalism, it is straightforward, but tedious to show that the spatial frequency of the ell configura-

tion is simply not suitable for reasonable image restoration of an extended source. The true centers of the two apertures in an ell are physically separated in two dimensions, with the result that, in the off-diagonal direction, there is a pronounced intermediate frequency peak in the spatial frequency response. Such a response, which is characteristic of a high resolution interferometer, cannot be reduced to a meaningful equivalent spatial frequency response, as defined by Eq. (25). Consequently, the ell configuration will not be considered as a possible element in a multiple-beam antenna for the ROMS mission.

We therefore conclude that reasonable image restoration can be achieved by restricting the configurational variation of the elements in a Mills cross multiple-beam antenna to the range between a symmetric cross (Figure 2a) and the unequal arm tee (Figure 2c). At the same time, some way must be found to compensate for the associated variation in the resolution and sensitivity of these elements.

## E. Non-Broadside Operation: Single Aperture Analysis

The ROMS mission requires a transverse beam swath at a 55 degree angle of incidence on the ocean surface, as is illustrated in Figure 1. This is to take advantage of the near independence of the vertically polarized radiation from the sea surface on roughness effects at this incidence angle and to obtain as large a surface emissivity as practical to increase the brightness temperature dependence on the physical temperature of the sea. Using a static Mills cross configuration, such a pattern can be achieved by appropriate phasing of the vertical arm, called

"coning". To illustrate this procedure, consider the specific example of the phased beam swing of a uniformly excited, vertically polarized aperture with dimensions $D_x$ and $D_y$ in the $x_\lambda$- and $y_\lambda$-directions, respectively. For large angle beam swings, the aperture polarization is important, and the general transform relationship given in Eq. (10) must be used. Then, according to the shift theorem, as given in Eq. (14), a uniform phase gradient of $m_o = -\cos\theta_o$ cycles per wavelength along the $y_\lambda$-direction of a uniformly excited aperture results in the vertically shifted far-field power radiation pattern

$$|E(\theta,\phi)|^2 = n_o \frac{(1-\ell^2)}{n} \operatorname{sinc}^2 [D_x \ell] \operatorname{sinc}^2 [D_y (m-m_o)] \quad . \tag{30}$$

This expression has been normalized to remove the dependence of the radiated power on aperture dimensions and input impedance, as discussed in Part C of this Section.

For a high directivity aperture ($D_x, D_y >> 1$), Eq. (30) has the approximate form in spherical coordinates

$$|E(\theta,\phi)|^2 \simeq \operatorname{sinc}^2 [(D_x \sin\theta_o) \sin\phi] \operatorname{sinc}^2 [(D_y \sin\theta_o)(\theta-\theta_o)]. \tag{31}$$

The corresponding total radiated power (beam solid angle, in this case) is

$$\Omega \simeq \frac{1}{D_x D_y \sin\theta_o} \quad . \tag{32}$$

As predicted, the effect of a vertical phase gradient is to project (cone) a fan shaped beam onto a horizontal surface at

the constant angle of incidence, $\theta_o$. Because of the phasing, the effective length of the aperture in the $y_\lambda$-direction is reduced by the factor sin $\theta_o$. The effective length in the $x_\lambda$-direction is also reduced by the same factor, but this is because it is referred to the horizontal beam angle, $\phi$, rather than to the true cone angle, $\phi'$, as defined in Figure 7.

Similar results are obtained for a transverse beam swing produced by a uniform phase gradient of $\ell_o = -\sin\theta_o \sin\phi_o$ cycles per wavelength along the $x_\lambda$-direction, i.e.,

$$|E(\theta,\phi)|^2 = \frac{n_o}{1-\ell_o^2}\,\frac{1-\ell^2}{n}\,\mathrm{sinc}^2\,[D_x(\ell-\ell_o)]\,\mathrm{sinc}^2\,[D_y m]$$

$$\simeq \mathrm{sinc}^2\,[(D_x\cos\phi_o)(\phi-\phi_o)]\,\mathrm{sinc}^2\,[D_y(\theta-\tfrac{\pi}{2})] \qquad (33)$$

and

$$\Omega \simeq \frac{1}{D_x D_y \cos\phi_o}\ . \qquad (34)$$

For this direction of beam swing, the effective length of the aperture in the $x_\lambda$-direction is reduced by the factor cos $\phi_o$.

The importance of the restriction $D_x, D_y >> 1$ in obtaining these simple results will now be examined. For this purpose, it is sufficient to consider the special case of a vertical beam swing along the polarization direction of an aperture where $D_x >> 1$, but the value of $D_y$ is left unrestricted. This represents a worst case, and the more general problem of an arbitrary beam swing with no directivity restrictions is not only more complicated, but provides no new insights. Then, for arbitrary values

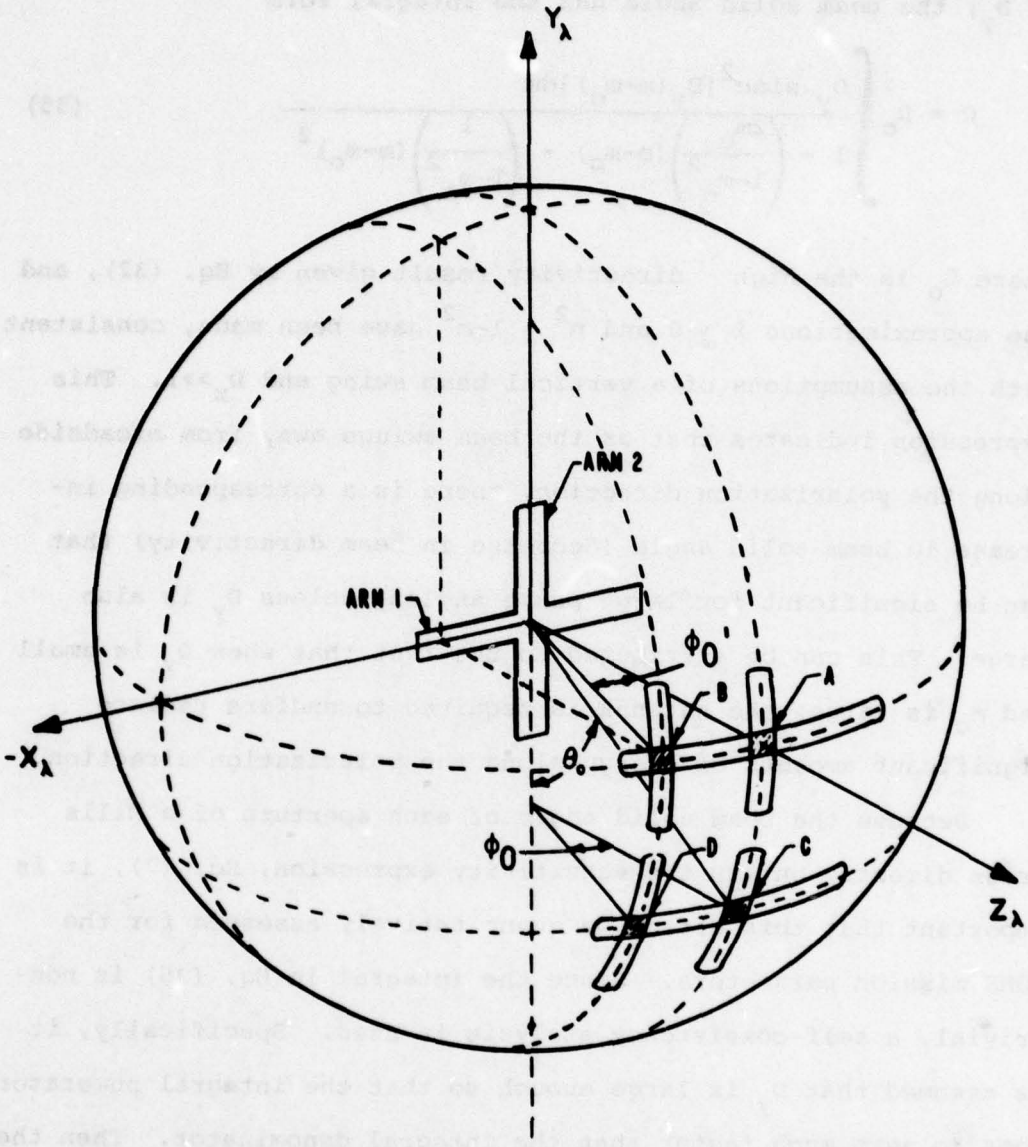


**Fig. 7 - Four different beam positions of the Mills cross: (A) broadside operation, (B) horizontal beam swing by phasing arm 1, (C) vertical beam swing by tilting arm 1 and phasing arm 2, and (D) general beam swing by tilting and phasing arm 1, and by phasing arm 2.**

of $D_y$, the beam solid angle has the integral form

$$\Omega = \Omega_o \int \frac{D_y \ \mathrm{sinc}^2[D_y(m-m_o)]dm}{1 - \left(\frac{2m_o}{1-m_o^2}\right)(m-m_o) - \left(\frac{1}{1-m_o^2}\right)(m-m_o)^2} \qquad (35)$$

where $\Omega_o$ is the high directivity result given by Eq. (32), and the approximations $\ell \simeq 0$ and $n^2 \simeq 1-m^2$ have been made, consistent with the assumptions of a vertical beam swing and $D_x >> 1$. This expression indicates that as the beam swings away from broadside along the polarization direction, there is a corresponding increase in beam solid angle (decrease in beam directivity) that can be significant for large phase angles, unless $D_y$ is also large. This can be attributed to the fact that when $D_y$ is small and $m_o$ is large, the antenna is required to endfire radiate significant amounts of energy along the polarization direction.

Because the beam solid angle of each aperture of a Mills cross directly enters the sensitivity expression, Eq. (7), it is important that this effect be quantitatively assessed for the ROMS mission parameters. Since the integral in Eq. (35) is non-trivial, a self-consistency analysis is used. Specifically, it is assumed that $D_y$ is large enough so that the integral numerator goes to zero much faster than the integral denominator. Then the denominator can be expanded and the integral evaluated to obtain the fractional increase in beam solid angle

$$\frac{\Delta\Omega}{\Omega_o} \simeq \frac{1}{\pi^2 D_y} \left[\frac{1}{1-m_o^2} + \left(\frac{2m_o}{1-m_o^2}\right)^2\right]. \qquad (36)$$

For the ROMS mission, $\theta_o \sim 50°$, which means $\Delta\Omega/\Omega \simeq 0.7/D_y$.

To satisfy the resolution and sensitivity requirements of the mission, it is anticipated that $D_y \gtrsim 30$ and $D_y \lesssim 3$ for the vertical and horizontal arms of the Mills cross, respectively. This means that there is less than a 2 percent error associated with phasing the vertical arm, but at least a 20 percent error if we try to phase the narrow dimension of the horizontal arm to produce a beam maximum at $\theta_o \simeq 50°$. Further, for this angle and $D_y \lesssim 3$, the self-consistency argument used to obtain Eq. (36) is violated. We conclude that large angle beam swings by phasing along the long dimensions of the arms of a Mills cross are acceptable, but that another procedure, such as mechanically tilting the arms, must be used to produce the required beam swings along the narrow dimensions.

## F. Non-Broadside Operation: Tilted-Arm Mills Cross

Figure 7 illustrates how the large angle beam swings required for the ROMS mission might be achieved by a combination of phasing the long dimensions and mechanically tilting the short dimensions of the arms of a Mills cross. Specifically, to produce a correlation maximum at a given position $(\theta_o, \phi_o)$, the following procedure is proposed:

- Phase the vertical arm length $L_2$ with a gradient $m_o = -\cos\theta_o$ cycles per wavelength to produce the horizontal fan beam centered at $(\theta_o, 0)$. From Eq. (32), the corresponding beam solid angle is $\Omega_2 = 1/(D_x D_y \sin\theta_o)$.
- Phase the horizontal arm length $L_1$ with a gradient

$\ell_o = -\sin\phi_o'$ cycles per wavelength to produce the vertical fan beam centered at $(0,\phi_o')$. From Eq. (34) the corresponding beam solid angle is $\Omega_1 = 1/(D_x D_y \cos\phi_o')$.

- Mechanically tilt the horizontal arm through an angle $\theta_o'$ about an axis through its center, parallel to the $x_\lambda$-direction, to produce the final correlation maximum centered at $(\theta_o,\phi_o)$.

By tilting the horizontal arm, the broadside directions of the vertical and horizontal arms are no longer the same; hence, the need to define the additional angles $\theta_o'$ and $\phi_o'$. These angles are shown in Figure 8, along with the specific relationships defining them in terms of $\theta_o$ and $\phi_o$. It should be noted that the correlation maximum is not necessarily centered at the peak power position of beam #2, which remains centered at $(\theta_o,0)$. This is intentional, since this is a characteristic of the multiple-beam Mills cross antenna utilizing a common vertical arm that is proposed in the next section.

The sensitivity of this configuration, as given by Eq. (7), is the convolution of the input signal with an effective antenna power pattern that is proportional to the product of the far-fields of each arm. To determine these far-fields, it is convenient to use two different coordinate systems, $(\theta,\phi)$ and $(\theta',\phi')$, referred to the broadside directions of the vertical and horizontal arms, respectively. Then, since the high directivity approximation is valid over the correlation region, Eqs. (31) and (33) are applicable, and the far-fields can be written

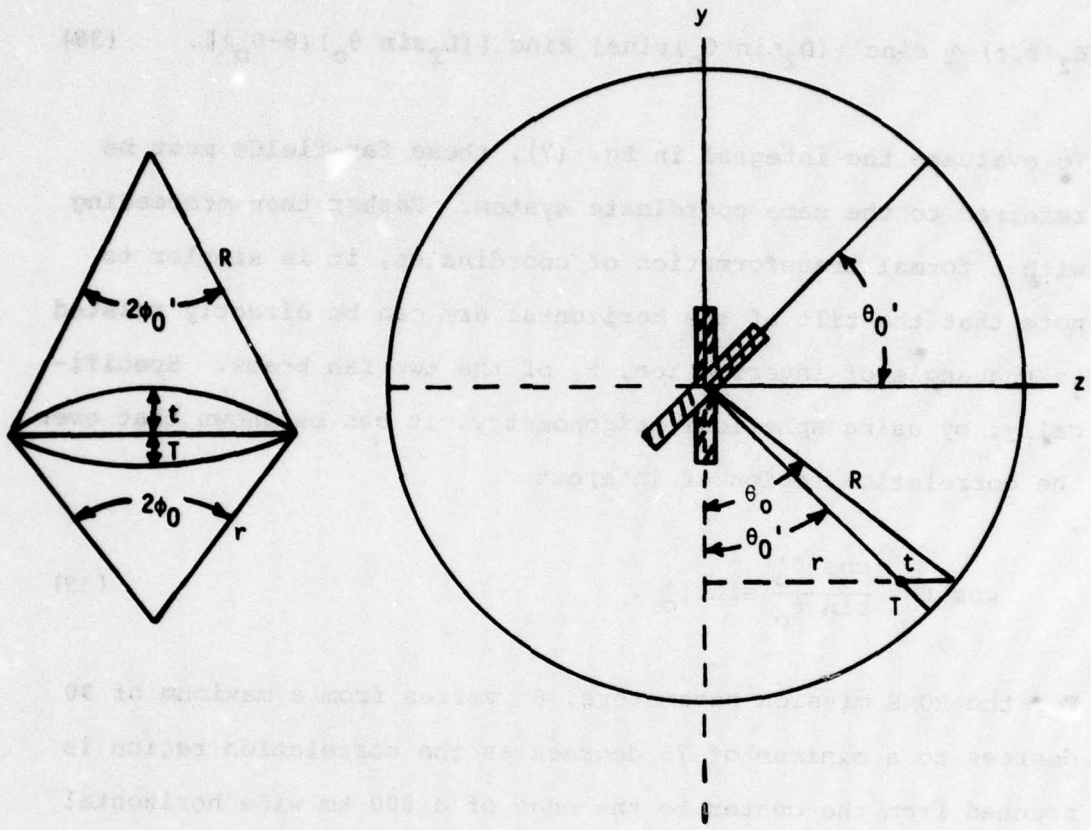


1. $\sin \phi_0' = \sin \theta_0 \sin \phi_0$

2. $$4 \sin^2\left(\frac{\theta_0 - \theta_0'}{2}\right) = \sin^2\theta_0(1 - \cos \phi_0)^2 + (1 - \cos \phi_0')^2 - 2 \sin \theta_0 \sin \theta_0' (1 - \cos \phi_0)(1 - \cos \phi_0')$$

**Fig. 8 - Angular relationships for the tilted-horizontal-arm antenna defining $\theta_o'$ and $\phi_o'$ in terms of $\theta_o$ and $\phi_o$ (see text)**

$$E_1(\theta',\phi') \simeq \text{sinc}\,[(L_1 \cos\phi_o')(\phi'-\phi_o')]\ \text{sinc}[D_1(\theta'-\tfrac{\pi}{2})], \qquad (37)$$

$$E_2(\theta,\phi) \simeq \text{sinc}\,[(D_2 \sin\theta_o)\sin\phi]\ \text{sinc}\,[(L_2 \sin\theta_o)(\theta-\theta_o)]. \qquad (38)$$

To evaluate the integral in Eq. (7), these far-fields must be referred to the same coordinate system. Rather than proceeding with a formal transformation of coordinates, it is simpler to note that the tilt of the horizontal arm can be directly related to the angle of intersection, $\beta$, of the two fan beams. Specifically, by using spherical trigonometry, it can be shown that over the correlation region of interest

$$\cos\beta \simeq \frac{\cos\theta_o'}{\sin\theta_o}\sin\phi_o' \ . \qquad (39)$$

For the ROMS mission parameters, $\beta$ varies from a maximum of 90 degrees to a minimum of 75 degrees as the correlation region is scanned from the center to the edge of a 500 km wide horizontal fan beam. Since both arms are vertically polarized, their far-fields are in planes parallel to the $y_\lambda z_\lambda$-plane, independent of tilts about the $x_\lambda$-axis. Therefore, the main effects of the decrease in the angle of intersection of the fan beams with increasing tilt of the horizontal arm are a reduction in effective arm length (a decrease in the transverse resolution) and an increase in the effective arm width (an increase in the correlation energy) through the same factor, sin $\beta$. Consequently, in the correlation region, the relationships between the two coordinate systems can be approximately written

$$\phi' - \phi_o' \cong \sin\beta \sin\theta_o(\phi-\phi_o), \tag{40}$$

$$\theta' - \frac{\pi}{2} \cong \frac{\theta-\theta_o}{\sin\beta}. \tag{41}$$

Using these relationships to transform the far-fields given by Eqs. (37) and (38) into the same coordinate system, the spatial frequency response of the tilted-arm Mills cross is determined in the usual manner by assuming a sinusoidal brightness temperature variation in the direction of interest, e.g.,

$$\Delta T(\theta,\phi) = \Delta T \cos 2\pi f_\theta(\theta-\theta_o) \quad \text{(longitudinal direction)} \tag{42}$$

or

$$\Delta T(\theta,\phi) = \Delta T \cos 2\pi f_\phi(\phi-\phi_o) \quad \text{(transverse direction)}, \tag{43}$$

and then evaluating the corresponding integral in Eq. (7). The result is the uniform spatial frequency response

$$T_s \cong 4\Delta T \operatorname{sinc}\left[(D_2\sin\theta_o)\sin\phi_o\right]\left[\frac{\frac{1}{L_1L_2\sin\theta_o\cos\phi_o'\sin\beta}}{\frac{1}{D_1L_1\cos\phi_o'} + \frac{1}{D_2L_2\sin\theta_o}}\right] \tag{44}$$

for

$$f_\theta < \frac{L_2\sin\theta_o - D_1/\sin\beta}{2} \quad \text{or} \quad f_\phi < \frac{L_1\sin\theta_o\cos\phi_o'\sin\beta - D_2\sin\theta_o}{2}.$$

The details of the shape of the spatial frequency cutoff have not been included here, since they are unimportant if $D_1$, $D_2 \ll L_1$, $L_2$.

In the ROMS mission the input signal results from brightness temperature variations of the ocean surface, which intercept the beam at the constant angle of incidence, $\theta_i$, as shown in Figure 1. Because of this oblique angle of incidence, the beam "footprint" on the ocean surface is elliptical, and there is an effective loss of resolution in the longitudinal direction. Equivalently, a sinusoidal temperature variation of the ocean surface in the longitudinal direction appears to occur at a higher angular spatial frequency than when the same spatial frequency is observed in the transverse direction, i.e.,

$$f_\phi = \sin\theta_o \cos\theta_i f_\theta \ . \tag{45}$$

To ensure a circular beam footprint (isotropic resolution), the dimensions of the arms of the Mills cross must be adjusted so that the two cutoff frequencies in Eq. (44) satisfy this relationship. The result of these adjustments is the uniform and isotropic spatial frequency response

$$T_s = 4\Delta T \ \mathrm{sinc}\left[D_{2e}\sin\phi_o\right] \frac{1}{L_e}\left\{\frac{D_{1e}D_{2e}}{D_{1e} + D_{2e}}\right\} \tag{46}$$

for

$$f_\phi \leq \frac{L_e}{2} \ ,$$

where the subscript "e" indicates that the dimensions are effective, and are defined by the relationships

$$L_e = L_1 \sin\theta_o \cos\phi_o' \sin\beta = L_2 \sin^2\theta_o \cos\theta_i \tag{47a}$$

$$D_{1e} = \frac{D_1 \sin\theta_o \cos\theta_i}{\sin\beta} \tag{47b}$$

$$D_{2e} = D_2 \sin\theta_o \, . \tag{47c}$$

Apart from the factor $\operatorname{sinc}\left[D_{2e} \sin\phi_o\right]$, which occurs because the correlation maximum does not in general coincide with the power maximum of the horizontal fan beam, Eq. (46) is identical in form to Eq. (24), which gives the broadside sensitivity of the symmetric Mills cross. The need for effective lengths is therefore a simple consequence of the non-broadside operation of a tilted antenna configuration that is used to isotropically monitor variations in a horizontal brightness temperature distribution.

## IV. Multiple-Beam Antenna Design and Analysis

### A. General Antenna Configuration

Based on the preceeding analysis, it is evident that a uniformly excited, tilted-horizontal-arm Mills cross, with a configurational variation limited to the range between a symmetric cross (Figure 2a) and a tee (Figure 2c), is the most promising structure for use as the basic element in a multiple-beam antenna designed for the ROMS application. The limit on the allowable range of configurational variations is necessary to ensure that the properties of each beam in the antenna are roughly equivalent, and are suitable for mapping an extended distribution, as discussed in Part D of the last Section. This limit also restricts the horizontal arm placement to the region defined by the vertical arm

length, $L_2$, and therefore limits the maximum antenna surface area to $\leq L_1 L_2$. It is a feature of the Mills cross unfilled aperture approach that the arm widths, and, hence, the antenna surface area, can be varied independently of the resolution. For a given set of mission requirements, this allows one to independently optimize the tradeoff between sensitivity, which is directly proportional to receiving area, and mission lifetime, which is adversely affected by a large surface area antenna. In the present analysis, only configurations with the maximum allowable area will be considered, in order to obtain upper limit estimates of antenna sensitivity. An example of such a configuration is shown in Figure 3, where the stacked arrangement of Mills crosses utilizes a single common vertical arm. Figure 9 illustrates the relationship between the average horizontal arm width, the vertical arm length, and the number of beams for this maximum area, tilted-arm configuration.

In this section, the details of the beam stacking procedure and some of the design tradeoffs that are involved in trying to construct such an antenna are presented. The performance of the basic configuration shown in Figure 3 is then calculated and analyzed in terms of the ROMS mission requirements. The effect of varying the number of vertical and/or horizontal arms on the predicted performance of this configuration is also examined.

## B. Beam Stacking Procedures

The general beam swing procedure outlined in Part F of Section III is used on each element in the configuration to stack the corresponding beams into the required high resolution 500 km transverse swath on the ocean surface. The details of this

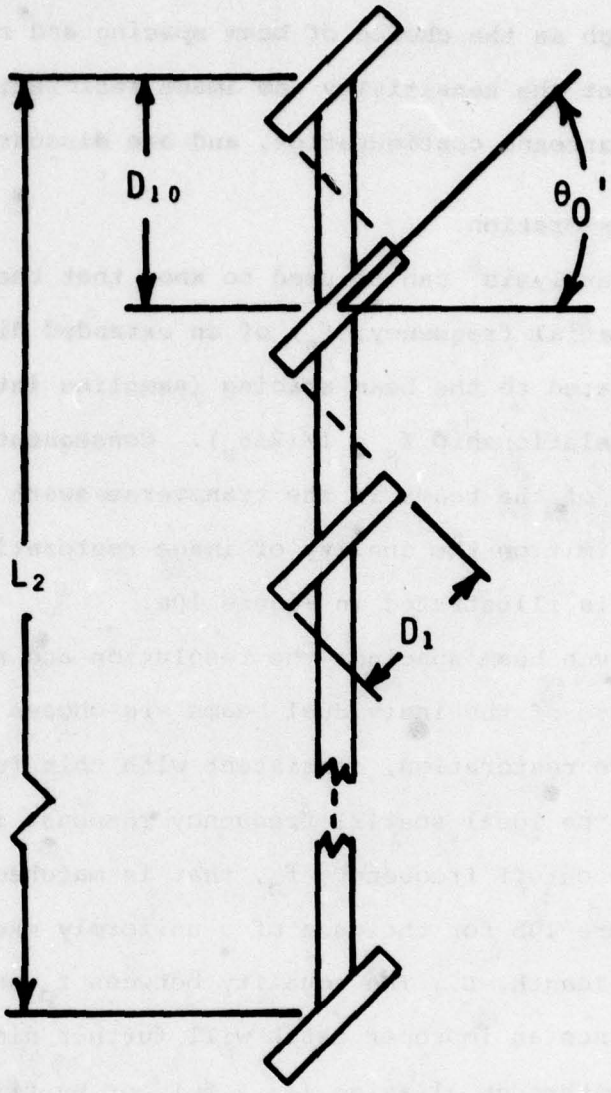


$$D_1 \text{ (ave)} = D_{10} \sin \theta_0' = \frac{L_2}{(\#\text{ beams} - 1)} \sin \theta_0'$$

**Fig. 9 - Relationship between average horizontal arm width, vertical arm length, and the number of beams for a maximum area tilted-arm configuration.**

procedure, such as the choice of beam spacing and resolution, directly affect the sensitivity and image restoration properties of the final antenna configuration, and are discussed below.

1. Image Restoration

Fourier analysis[9] can be used to show that the maximum observable spatial frequency, $f_s$, of an extended distribution, $T_B(\phi)$, is related to the beam spacing (sampling interval), $\Delta\phi_s$, through the relationship $f_s = 1/(2\Delta\phi_s)$. Consequently, the discrete spacing of the beams in the transverse swath places a fundamental limit on the quality of image restoration achievable. This concept is illustrated in Figure 10a.

For a given beam spacing, the resolution and spatial frequency response of the individual beams are chosen so as to optimize image restoration, consistent with this fundamental limitation. The ideal spatial frequency response is one that is flat out to a cutoff frequency, $f_c$, that is matched to $f_s$, as shown in Figure 10b for the case of a uniformly excited Mills cross of arm length, L. The equality between $f_c$ and $f_s$ is important, since an improper match will further distort the image, either through aliasing ($f_c > f_s$), or by filtering ($f_c < f_s$). It should be pointed out that an ideal rectangular spatial frequency response corresponds to a sinc function real space power pattern, as shown in Figure 10b. Because it involves both positive and <u>negative</u> sidelobes, this particular power pattern is unique to phase-switched interferometers such as the Mills cross, and cannot be achieved with conventional antennas.

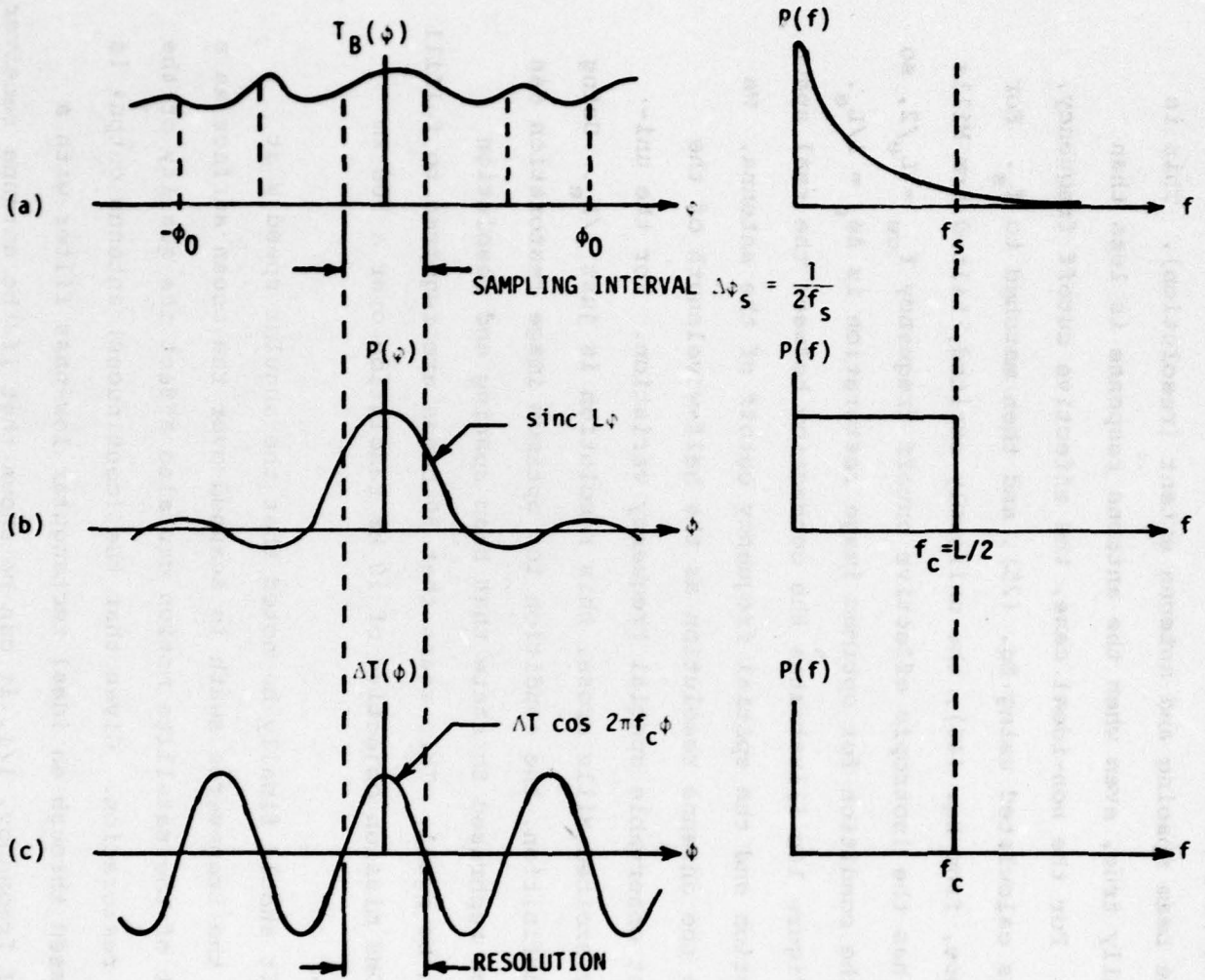


**Fig. 10 - Examples of real space and spatial frequency distributions for (a) ocean brightness temperature, (b) antenna power pattern, and (c) the spatial frequency cutoff component of $T_B$ ($\phi$)**

Note that for this particular ideal case, $f_c = L/2$, so that the frequency matching condition establishes the relationship between beam spacing and antenna extent (resolution). This is generally true, even when the antenna response is less than ideal. For the non-ideal case, the effective cutoff frequency, $f_{ce}$, is calculated using Eq. (25), and then matched to $f_s$. For instance, from Eq. (46), the uniformly excited, tilted arm Mills cross has the isotropic effective cutoff frequency $f_{ce} = L_e/2$, so that the condition for optimum image restoration is $\Delta\phi_s = 1/L_e$.

Figure 10c illustrates the connection between the real space resolution and the spatial frequency cutoff of the antenna. We define the antenna resolution as the half-wavelength of the highest observable spatial frequency variation. For the uniformly excited Mills cross, this resolution is just $1/L_e$. Using this definition, the condition for optimum image restoration can then be rephrased to state that beam spacing and resolution should be equal. This means that 50 beams are required to fulfill the ROMS mission objective of 10 km resolution over a 500 km swath.

It should finally be noted that the angular speed $\omega$ at which the transverse swath is scanned over the ocean surface as a result of the satellite motion can also affect the quality of the image restoration. Given that the (continuous) antenna output is processed through an ideal rectangular low-pass filter with a cutoff frequency, $1/\tau$, it can be shown that if the antenna receiver response time is short compared to $\tau$ <u>and</u> if $\omega\tau \leq \Delta\phi_s$, then there is no additional loss in image quality due to the satellite motion.

Therefore, $\tau$, which is just the effective antenna integration time, should not exceed the time it takes the swath to move forward over the ocean surface one beam spacing.

2. Sensitivity

A design option of the Mills cross multiple-beam antenna is that each vertical arm can be used in common with several horizontal arms to form the multiple-beam swath. Full utilization of this option considerably reduces the antenna size and complexity. Figure 3 illustrates the extreme case of a single vertical arm configuration. The primary limitation on multi-beaming the vertical arms is beam sensitivity. In particular, two independent mechanisms act to reduce sensitivity:

- Configuration Variation. Only one of the horizontal arms can be placed in the fully symmetric position with respect to a common vertical arm. As was shown in Part D of Section III, there is an asymmetric increase in resolution and a corresponding drop in sensitivity as the horizontal arm is moved off center. Since the vertical arm is common, its dimensions cannot be varied to compensate for this effect. The result is a steady drop in sensitivity up to a maximum factor of two as the configuration varies from a symmetric cross (Figure 2a) to a tee (Figure 2c). This effect is illustrated by a curve A in Figure 11.

- Asymmetric Beam Stacking. Only one of the horizontal arm beams can occupy the peak amplitude position of the

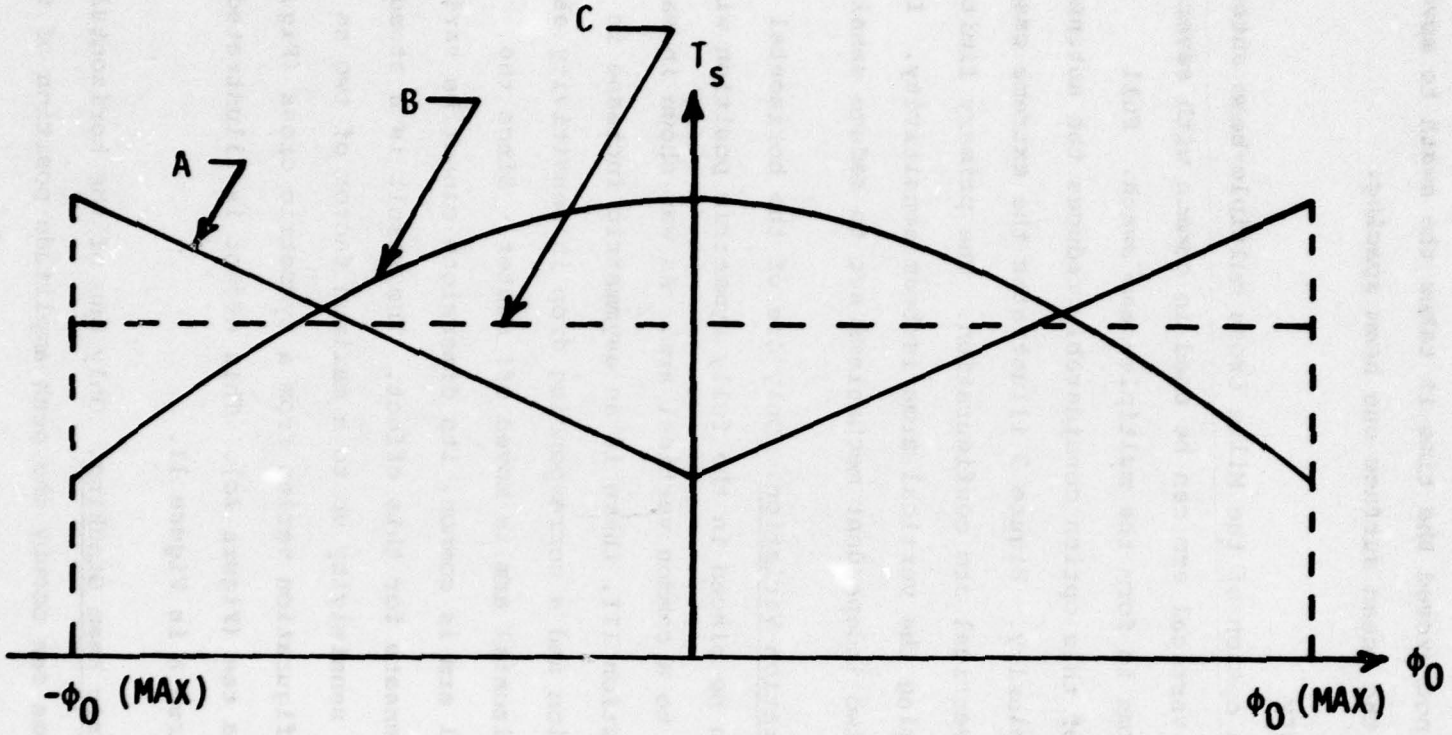


Fig. 11 - Sensitivity variation as a function of beam position due to the configurational variation (Curve A) and the beam stacking variation (Curve B) when one vertical arm is used in the tilted-arm, multiple-beam antenna. By using the appropriate design procedure, these two sensitivity variations can be made to roughly cancel (Curve C)

vertical arm beam. By phasing and tilting the horizontal arms as specified above, the beams can be optimally stacked according to sampling theory, but there is a steady roll-off in sensitivity with beam position relative to the maximum. Specifically, if $\phi_o$ is the horizontal angular deviation of a given beam from the peak position, and $D_{2e}$ is the effective width of the vertical arm, Eq. (46) indicates that $T_s(\phi_o) = T_s(0)\text{sinc}\,[D_{2e}\sin\phi_o]$. This roll-off of sensitivity with beam position is illustrated by curve B in Figure 11 for the case of one vertical arm.

By using the appropriate design procedure, these two sensitivity variations can be made to roughly cancel, as is illustrated by curve C in Figure 11. Specifically, $D_{2e}$ is chosen so that $\text{sinc}[D_{2e}\sin\phi_o(\text{max})] = 0.5$. Then the phasings of the horizontal arms are chosen so that the low-sensitivity tee configuration beams are pointed at $\phi_o \simeq 0$, while the full-sensitivity cross configuration beams are pointed at $\phi_o \simeq \phi_o(\text{max})$. Using this design procedure, the horizontal arms are of equal width. Unfortunately, there is no simple way to also remove the configuration variation of the resolution, so there will be some data aliasing with this configuration.

By going to more than one vertical arm, the sensitivity roll-off due to asymmetric beam stacking can be reduced. For example, the vertical arms of a two arm system are first rotated in opposite directions about a vertical axis to produce vertical beam maximums at $\pm\,\phi_{BM}$, where $\phi_{BM} = \phi_o(\text{max})/2$. Then, if half the

horizontal arms are paired with each vertical arm, the sensitivity expression for each set is $T_s(\phi_o) = T_s(\phi_{BM})\text{sinc}[D_{2e}\sin(\phi_o - \phi_{BM})]$. Although the detailed design procedure for balancing this sensitivity variation against the configuration variation is more complicated, it is not fundamentally different from the procedure proposed for the single vertical arm system.

C. Antenna Noise Temperature

The noise temperature of the phase-switched Mills cross can be written[12]

$$T_N = \frac{2(T_{RT} + T_B(\text{ave}))}{\sqrt{\Delta\nu\tau}}, \tag{48}$$

where $\tau$ is the integration time (1.4 seconds at 10 km resolution), $\Delta\nu$ is the receiver pre-detection bandwidth (500 MHz), $T_B(\text{ave})$ is the average background brightness temperature (150°K at 6 GHz), and $T_{RT}$ is the combined noise temperature of the receiver and of the transmission lines (290°K). The values in parentheses are appropriate to the ROMS application. A corporate fed, waveguide antenna structure has been assumed, so that transmission line losses at 6 GHz can be neglected[2]. It should be emphasized that the maximum allowable integration time, as determined by image restoration considerations, is directly proportional to the antenna resolution.

D. Antenna Design Chart

The design details of three different Mills cross multiple-beam antennas, and their predicted performances in terms of the ROMS mission requirements, are presented in Figure 12. All

| Configuration | A | B | C |
|---|---|---|---|
| Vertical Arms | 1 | 1 | 2 |
| Horizontal Arms (Number of Beams) | 50 | 25 | 50 |
| Sampling Interval (km) | 10 | 20 | 10 |
| Beam Angle, $\phi_0$ (maximum) | $22.7^0$ | $22.2^0$ | $22.7^0$ |
| Beam Interval, $\Delta\phi_0$ | $0.93^0$ | $1.85^0$ | $0.93^0$ |
| Major Beam Angle, $\phi_0'$ (maximum) | $17^0$ | $16.7^0$ | $17^0$ |
| Tilt Deviation ($\theta_0$-$\theta_0'$)(maximum) | $2.3^0$ | $2.3^0$ | $2.3^0$ |
| Beam Intersection Angle, $\beta$ (minimum) | $75^0$ | $75^0$ | $75^0$ |
| Vertical Beam Peak, $\phi_{BM}$ | $0^0$ | $0^0$ | $\pm 11.5^0$ |
| Effective Length, $L_e$ | $62\lambda$ | $31\lambda$ | $62\lambda$ |
| Effective Horizontal Width, $D_{1_e}$ | $1.25\lambda$ | $1.3\lambda$ | $1.25\lambda$ |
| Effective Vertical Width, $D_{2_e}$ | $1.55\lambda$ | $1.6\lambda$ | $3.1\lambda$ |
| Vertical Height, $L_2$(m) | 9.35 | 4.68 | 9.35 |
| Horizontal Width, $L_1$(m) | 4.08→4.42 | 2.04→2.21 | 4.08→4.42 |
| Vertical Arm Width, $D_2$(m) | 0.10 | 0.11 | 0.20 |
| Horizontal Arm Width, $D_1$(m) | 0.14 | 0.15 | 0.14 |
| $T_S(m^0K)$ | 11 | 23 | 14 |
| $T_N(m^0K)$ | 33 | 23 | 33 |
| S/N | 0.3 | 1.0 | 0.4 |

ROMS tilted-arm antenna design chart for the given mission parameters:

| $h_0$ | SWATH | $\theta_i$ | $\theta_0$ | r | R | $\lambda$ | $\Delta T$ |
|---|---|---|---|---|---|---|---|
| 500 km | 500 km | 55° | 49.4° | 619 km | 815 km | 5 cm | 0.5°K |

**Fig. 12 - Three possible designs of a Mills cross multiple-beam antenna, and their predicted performances in terms of the ROMS mission requirements shown**

three configurations are similar in design, differing only in the number of horizontal and/or vertical arms. Configuration B is illustrated in Figure 3. There are so many design degrees of freedom that the three configurations chosen are meant to be a representative rather than a complete set of the full range of possibilities. Figure 13 shows the complicated tradeoffs that must be made in trying to establish the optimum antenna design, and it is evident that there is probably no unique solution.

## V. Discussion and Conclusions

Based on the preceeding analysis and the design chart in Figure 12, the following observations can be made:

- It is not possible to meet the full ROMS mission requirements using a Mills cross multiple-beam antenna. Configurations A and C, which are designed for 10 km resolution, have signal-to-noise ratios well below an acceptable value. In addition, rough calculations indicate that a waveguide-fed antenna of this size cannot meet the weight restrictions and the minimal lifetime requirements of the ROMS mission without using fabrication techniques beyond the present state-of-the-art.

- The overall sensitivity advantage of two vertical arms (Configuration C) over a single vertical arm (Configuration A) is not large enough to justify dealing with the additional design complexity. The relatively small advantage of

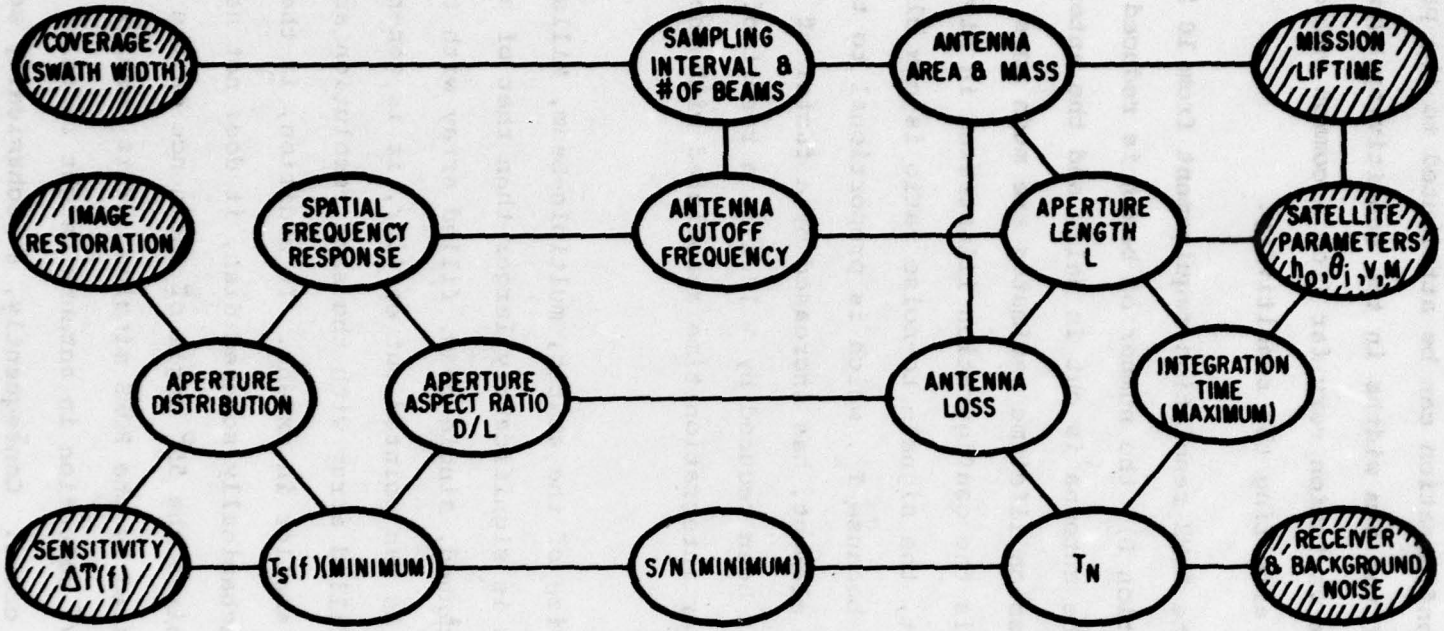


Fig. 13 - Design and sizing chart illustrating the complicated tradeoffs that must be made in trying to optimize the performance of a Mills cross multiple-beam antenna. The cross-hatched bubbles at either end of this diagram represent the given parameters.

the two-arm configuration can be attributed to the parallel combination of the arm widths in the sensitivity expression which prevents variation very far from a common value without adversely affecting the sensitivity.

- By relaxing the ROMS resolution requirement from 10 km to 20 km (Configuration B), the number of beams is reduced to 25, the size of the antenna is cut in half, and the antenna weight and mission lifetime estimates are much more acceptable. This is the configuration illustrated in Figure 3. More important, the signal- to-noise ratio is now close to one. This is because $T_s$, which is proportional to the D/L ratio of each element, has increased by a factor of two, and because $T_N$ has been reduced by $\sim 1/\sqrt{2}$ as a result of the longer receiver integration time associated with the lower resolution.

- The overall size of the static, multiple-beam, Mills cross configuration is significantly larger than that of a mechanically scanned, single-beam, filled array with the same resolution. As was pointed out earlier, it is generally true that a filled array with the same resolution as a Mills cross is $\sim\sqrt{2}$ smaller in extent. In addition, if the filled array is a mechanically scanned dish, it does not need to be phased to achieve the $55^{\circ}$ angle of incidence on the ocean surface required by the ROMS mission. This results in an additional $\sim\sqrt{2}$ reduction in antenna height relative to the phased Mills cross. Consequently, a mechanically scanned

dish with an area almost a factor of three smaller than that of the static Mills cross configuration should satisfy the resolution requirements of the ROMS mission. This is a significant consideration in weighing the two alternatives.

- In the preceeding analysis, it has been assumed that the properties of each beam in the multiple-beam configuration can be treated independently. In fact, mechanical shadowing and mutual coupling[10,11] can introduce significant pertubations, and should be considered in any careful analysis. However, it is antiticipated that these pertubations are considerably smaller than those encountered in dealing with the other types of multiple-beam configurations, where beam interference and crosstalk are known to be major problems[6]. Therefore, in this initial study, the mutual coupling and other interactions between the Mills cross elements have been neglected.

In summary, the Mills cross configuration does not completely meet the stated requirements of the ROMS application. However, its mechanical and conceptual simplicity relative to alternative antenna configurations make it an attractive candidate for applications where the sensitivity requirement for a given resolution is less severe. Applications which involve relatively strong small sources and where spatial resolution is more important than signal-to-noise considerations are ideal for the Mills cross approach. In such cases, full advantage can be taken of the unfilled aperture property of the Mills cross (i.e., resolution

and sensitivity can be varied independently) in order to achieve the required sensitivity-resolution combination with minimum antenna area and weight. Even in a case such as the ROMS application, where this advantage is less evident, the design and analysis of the Mills cross multiple-beam antenna provide a useful frame of reference for (1) assessing the relative importance of each of the mission parameters in terms of their impact on antenna design and predicted performance, (2) evaluating alternative antenna configurations and operating modes, and (3) illustrating some of the design tradeoffs and general problems that are encountered in trying to map an extended source from a space platform.

## REFERENCES


1. "Scientific Uses of the Space Shuttle," Shuttle Board, National Research Council, National Academy of Sciences, Washington, DC, 1974.

2. C. A. Levis and H. C. Lin, "System Implications of Large Radiometric Array Antennas," IEEE Trans. Microwave Theory Tech., Vol. MTT-25, pp. 248-253, 1977.

3. B. Y. Mills and A. G. Little, "A High Resolution Aerial System of a New Type," Australian J. Phys., Vol. 6, pp. 272-278, 1953; B. Y. Mills, "Cross-type Radio Telescopes," Proc. I.R.E. (Australia), Vol. 24, pp. 132-140, 1963.

4. W. H. Peake, "Interaction of Electromagnetic Waves with Some Natural Surfaces," IRE Trans. on Antennas and Propagation (Special Suppl.), Vol. AP-7, pp. S324-S329, December 1959.

5. J. P. Hollinger, "Passive Microwave Measurements of Sea Surface Roughness," IEEE Trans. Geoscience Elect., Vol. GE-9, pp. 165-169, July 1971.

6. J. L. Butler, "Digital, Matrix, and Intermediate-Frequency Scanning," Microwave Scanning Antennas, Chap. 3, Vol. III, H. C. Hansen (ed.), Academic Press Inc., New York, 1966.

7. H. C. Ko, "Radio Telescope Antennas," Microwave Scanning Antennas, Chap. 4, Vol. I, H.C. Hansen (ed.), Academic Press Inc., New York, 1964.

8. J. Brown, "A Theoretical Analysis of Some Errors in Aerial Measurements," Proc. Inst. Elec. Engrs. (London), Vol. 105C, pp. 343-351, 1958.

9. R. N. Bracewell, The Fourier Transform and Its Applications, McGraw-Hill Book Company, New York, 1965.

10. H. A. Wheeler, "Simple Relations Derived from a Phased-Array Antenna Made of an Infinite Current Sheet," IEEE Trans. Antennas Propagation, Vol. AP-13, pp. 506-514, 1965.

11. A. A. Oliner and R. G. Malech, "Mutual Coupling of Infinite Scanning Arrays," Microwave Scanning Antennas, Chap. 3, Vol. II, H. C. Hansen (ed.), Academic Press Inc., New York, 1966.

12. J. D. Kraus, Radio Astromony, McGraw-Hill Book Company, New York, 1966.